Optical Vector Wave Mixing Processes in Nonlinear Birefringent Nematic Liquid Crystals

H. J. Eichler, G. Hilliger, R. Macdonald, and P. Meindl
Optical Institute of the Technical University of Berlin, Strasse des 17. Juni 135, D-10623 Berlin, Germany
(Received 3 February 1997)

Optical vector wave mixing processes in nematic liquid crystals as a birefringent nonlinear medium have been investigated. Experimental results are explained theoretically taking into account the polarization dependence of the wave mixing effect and the tensor properties of the nonlinearity. [S0031-9007(97)03376-0]

PACS numbers: 42.70.Df, 42.65.Hw

Degenerate optical wave mixing is a well known phenomenon that occurs in different optically nonlinear media like photorefractive oxides, liquid crystals, or Kerr media [1]. One interesting feature of these processes is the possibility of energy exchange between two mixing beams which is naturally obtained, e.g., in photorefractive media as a consequence of an intrinsic phase shift of $\pi/2$ between the optical interference pattern and the refractive index grating. On the contrary, Kerr-like media are locally nonlinear and do not show such a phase shift. Nevertheless, energy transfer by two-wave mixing in Kerr-like media may be obtained under certain conditions, e.g., in nonlinear layers with small interaction length compared to the grating period by means of higher order scattering waves [2–4], or transient wave mixing resulting in a dynamic phase shift between the interference and index grating [5,6]. Recently, new wave mixing processes with the feasibility of optical amplification and polarization switching in birefringent optically nonlinear media due to vectorial coupling of beams with arbitrary polarizations has been predicted [7–10]. In the present paper, such polarization dependent wave mixing processes using nematic liquid crystals as a nonlinear medium are investigated experimentally for the first time. The relevant optical nonlinearity was the photothermic change of the refractive index, which is much higher than in most other media and has the interesting feature that the sign of the nonlinear coefficients depend on the polarization of the light [11].

Figure 1 shows a scheme of the investigated wave mixing geometry. The notation are chosen similar to those of the theoretical treatment of Khoo [7]. Because of the birefringence of the nonlinear material extraordinarily (e) and ordinarily (o) polarized waves propagate inside the liquid crystal, which are denoted by E_1 and E_2 in the case of the signal beam and by E_3 and E_4 for the pump beam. Pump and signal beams are assumed to be plane waves in the following. The intensity of the e and o beams inside the liquid crystal are then given by

$$|\vec{E}_e|^2 = (|\vec{E}_1|^2 + |\vec{E}_3|^2) + (\vec{E}_1 \cdot \vec{E}_3^* e^{i\vec{q}_e\cdot\vec{r}} + \text{c.c.}), \quad (1)$$

$$|\vec{E}_o|^2 = (|\vec{E}_2|^2 + |\vec{E}_4|^2) + (\vec{E}_2 \cdot \vec{E}_4^* e^{i\vec{q}_o\cdot\vec{r}} + \text{c.c.}), \quad (2)$$

with the grating vectors $\vec{q}_e = \vec{k}_1 - \vec{k}_3$ and $\vec{q}_o = \vec{k}_2 - \vec{k}_4$. The intensity of both components will cause a change in the temperature $\Delta T = \Delta T_e + \Delta T_o$ due to absorption. The total rise in temperature ΔT leads to a change of the refractive indices, which can be approximated by

$$\Delta n_{e,o} = (dn_{e,o}/dT)\Delta T\,. \quad (3)$$

The interaction of the four waves in the nonlinear medium mediated by these index changes may then be calculated within the slowly varying envelope approximation of the Maxwell's equations which yields a system of four coupled differential equations (see Ref. [7]). In the following, we will discuss the particular case that we have two strong pump waves $E_{3,4}$ compared to the weak signal waves $E_{1,2}$, with respect to our experimental situation. Therefore, the pump waves are assumed to be not depleted by the wave mixing process and the only effect of nonlinearity upon $E_{3,4}$ is a homogeneous self-modulation in the optical phase, which can be written as $\vec{E}_{3,4} = \vec{E}_{3,4}(0)e^{i\Phi_{3,4}z}$ with

$$\Phi_3 = \frac{\omega^2 n_e}{k_{3z}c_0^2}\,(n^s_{e,e}|E_3|^2 + n^s_{e,o}|E_4|^2)\,, \quad (4)$$

$$\Phi_4 = \frac{\omega^2 n_o}{k_{4z}c_0^2}\,(n^s_{o,e}|E_3|^2 + n^s_{o,o}|E_4|^2)\,. \quad (5)$$

This homogeneous self-phase modulation has to be considered in the calculation of the wave mixing process, as will be shown below. The coefficients $n^{s,q}_{i,j}$ are given by $n^{s,q}_{i,j} = (dn_i/dT)(\alpha_j\tau^{s,q}_j/\rho c Z_j)$ with $i, j \in \{e, o\}$; ρ,

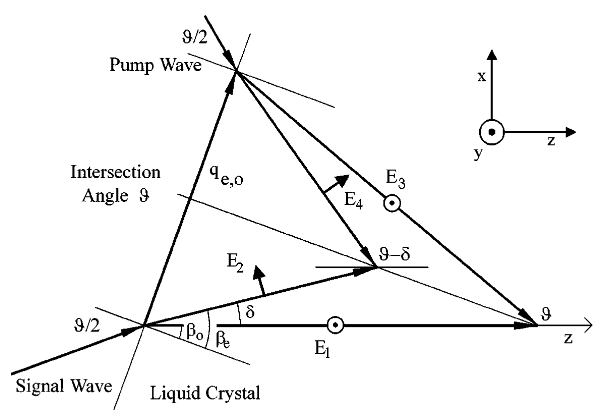

FIG. 1. Scheme of the investigated wave mixing geometry inside the liquid crystal. Birefringence leads to different wave components for the pump and the signal beams.

mass density; c, heat capacity; and Z_j, wave impedance. The grating part of the refractive index change is denoted by an index q and the homogeneous part by s, respectively. The absorption coefficients for different polarizations are denoted by α_j, and $\tau_j^{s,q}$ are the characteristic time constants for the s or the q part of the temperature distribution. In our experiments we used laser pulses of about $\tau^p = 2-20$ ms duration. Since we have $\tau_{e,o}^q = 0.8$ ms in our experiments, the index grating reaches the stationary state within the laser pulse. On the contrary, the homogeneous part has a characteristic diffusion time of about 200 ms determined by the finite beam diameter. Therefore we have to set $\tau_j^s = \tau^p$.

The relevant differential equations which describe the nonlinear intensity changes of the waves E_1 and E_2 may then be reduced to the following form:

$$\frac{\partial E_1}{\partial z} = i(\Phi_1 E_1 + \gamma_1 E_2 e^{i\Delta z}), \tag{6}$$

$$\frac{\partial E_2}{\partial z} = i(\Phi_2 E_2 + \gamma_2 E_1 e^{-i\Delta z}), \tag{7}$$

with $\Delta = \Phi_3 - \Phi_4$ and

$$\Phi_1 = \frac{\omega^2 n_e}{k_{1z} c_0^2} (2n_{e,e}^s |E_3|^2 + n_{e,o}^s |E_4|^2), \tag{8}$$

$$\Phi_2 = \frac{\omega^2 n_o}{k_{2z} c_0^2} \left[n_{o,e}^s |E_3|^2 + \left(n_{o,o}^s - n_{o,o}^q \frac{\cos(\vartheta - \delta)\cos(2\beta_o)}{\cos\delta} \right) |E_4|^2 \right], \tag{9}$$

$$\gamma_1 = \frac{\omega^2 n_e}{k_{1z} c_o^2} n_{e,o}^q E_3 E_4^* e^{i\Delta\vec{k}\cdot\vec{r}} \cos(2\beta_o), \tag{10}$$

$$\gamma_2 = \frac{\omega^2 n_o}{k_{2z} c_o^2} n_{o,e}^q E_3^* E_4 e^{-i\Delta\vec{k}\cdot\vec{r}} \frac{\cos(\vartheta - \delta)}{-\cos\delta}, \tag{11}$$

where $\Delta\vec{k} = \vec{q}_o - \vec{q}_e$ is the mismatch between the gratings induced by o and e beams, respectively. Introducing $\beta = \frac{1}{2}(\Phi_2 - \Phi_1 + \Delta)$ and $g = \sqrt{|\beta^2 + \gamma_1\gamma_2|}$ the solution of Eqs. (6) and (7) are given in case 1 ($\beta^2 + \gamma_1\gamma_2 < 0$) by

$$E_1(z) = e^{(i/2)(\phi_1+\phi_2+\Delta)z} \left[E_1(0) \left(\cosh(gz) - i\frac{\beta}{g}\sinh(gz) \right) + E_2(0) i \frac{\gamma_1}{g} \sinh(gz) \right], \tag{12}$$

$$E_2(z) = e^{(i/2)(\phi_1+\phi_2-\Delta)z} \left[E_2(0) \left(\cosh(gz) + i\frac{\beta}{g}\sinh(gz) \right) + E_1(0) i \frac{\gamma_2}{g} \sinh(gz) \right]. \tag{13}$$

In case 2 ($\beta^2 + \gamma_1\gamma_2 > 0$) sinh and cosh are replaced by sin and cos, respectively. However the amplitudes $E_i(0)$ may include an initial phase φ_i, which allows one to describe the polarization of the beams at the input face of the sample. The main difference is that in case 1 the signal beam components are amplified by the pump waves E_3 and E_4, whereas in case 2 the power oscillates periodically between the two signal beam components E_1 and E_2. In our case the thermo-optic nonlinear effect has different signs in the nonlinear coefficients, depending on the polarization of the waves. As a consequence $\gamma_1\gamma_2$ is always negative, whereas β^2 has a positive sign. Both terms depend on several parameters and are of the same magnitude in our experimental geometry, so that both cases must be considered. In the experiments shown in Fig. 2, we have, e.g., a periodic alternation between both cases. However, if gz is rather small, the trigonometric and hyperbolic functions can be approximated, leading to a common solution for the two cases.

For our experimental investigations we used the chopped linear polarized beam of a cw Ar laser at 514.5 nm wavelength with pulse durations between 2 and 20 ms. A beam splitter was used to get the signal and pump beams. The two beams were focused to a diameter of about 170 μm into the liquid crystal cell. The intersection angle was about 10.5 mrad. The 100 μm thick, planarly oriented liquid crystal was 5CB (pentyl-cyanobiphenyl) doped with a dichroic dye ($\approx$3 wt. % D37 from Merck) to increase the absorption to $\alpha_o = 2000\ \text{m}^{-1}$ and $\alpha_e = 9000\ \text{m}^{-1}$. The main effect connected with this anthraquinone-dye is enhanced photoheating, since these dyes do not show photoisomerization like, e.g., azo-dyes. Furthermore, it must be noted that we did not observe any optical reorientation effect in our experiments, which have been observed with some particular anthraquinone-dyes in

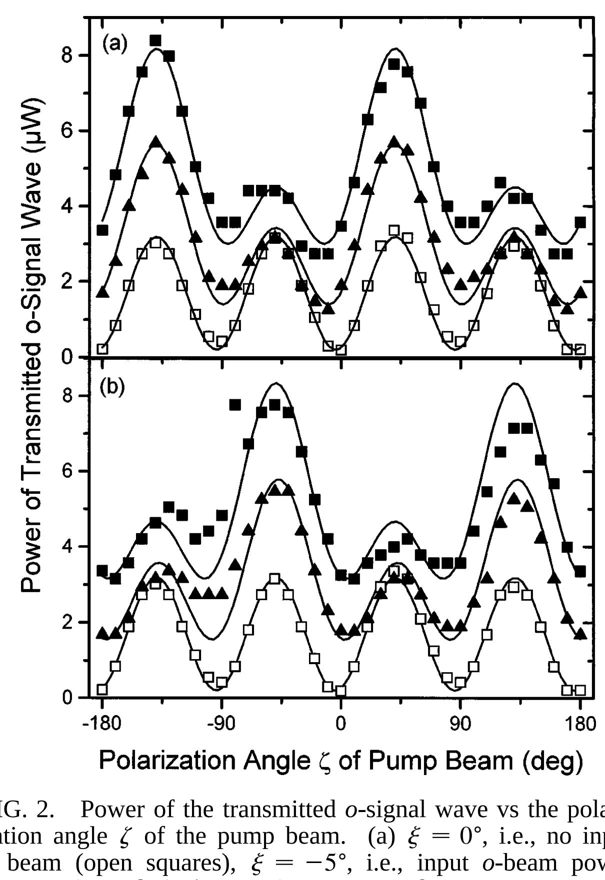

FIG. 2. Power of the transmitted o-signal wave vs the polarization angle ζ of the pump beam. (a) $\xi = 0°$, i.e., no input o beam (open squares), $\xi = -5°$, i.e., input o-beam power 3.2 μW (triangles), $\xi = -8°$, i.e., input o-beam power 5.1 μW (squares). (b) Same, but $\xi = 0°, +5°, +8°$. Solid curves display theoretical calculations.

other investigations. The thermal index gradients at $T_{\mathrm{NI}} - T = 10\ \mathrm{K}$ are $dn_o/dT = 0.8 \times 10^{-3}\ \mathrm{K}^{-1}$ and $dn_e/dT = -6.5 \times 10^{-3}\ \mathrm{K}^{-1}$.

The *e* and *o* components of the waves as well as higher order scattered waves were measured with *p*-*i*-*n* photodiodes behind a polarizer. The input signal wave was mainly extraordinarily polarized (i.e., parallel to the optical axis of the liquid crystal) and contained only a small ordinary component and, in general, we measured changes in this ordinary component E_2. We define ξ and ζ as the angles between the direction of the optical axis of the liquid crystal and the direction of the polarization of the signal and the pump wave, respectively. Half-wave plates were used to vary these angles and in that way the relative amplitudes of the *e* and *o* components. The dynamics of the transmitted ordinary signal wave show typical thermal grating buildup times of about 0.8 ms, and the pump duration was chosen long enough to ensure stationary gratings. At higher intensities unwanted self-focusing caused by strong self-phase modulation of the pump waves leads to direct diffraction into the direction of the signal wave. In order to avoid this effect laser powers below 4.5 mW have been used.

Let us first investigate the case when there is no ordinary input signal wave, i.e., $E_2(0) = 0$. The lowest plots in Fig. 2 show the transmitted power of the *o*-signal beam depending on the angle of polarization of the pump beam ζ. If there is no ordinary input signal wave, the corresponding ordinary output increases and decreases periodically with maxima at pump orientations of $\zeta = \pm 45°, 135°$, etc. The observed behavior can be explained simply by diffraction of the ordinary component of the pump beam E_4 at the grating written by the extraordinary beams E_1 and E_3, which was also symmetric for the $\pm$ first diffraction order.

The situation becomes clearly different for the nonvanishing ordinary component of the input signal beam E_2 ($\xi \neq 0$). The results are also shown in Fig. 2. With increasing ordinary input component of the signal wave the periodic dependence of the transmitted power becomes asymmetric. It is an interesting point that this asymmetry depends on the sign of the input signal wave amplitude, which is a clear indication that the vector characteristic of the mixing beams is really important. To understand the effect we calculate the power of the signal beam using Eq. (13).

$$P_2(z) \propto E_2(z)E_2^*(z) = |E_2(0)|^2 \times \left(\cosh(gz) + \frac{\beta^2}{g^2}\sinh^2(gz)\right) + |E_1(0)|^2\frac{|\gamma_2|^2}{g^2} \times \sinh^2(gz) + \mathrm{Re}[\gamma_2 E_1(0)E_2^*(0)]\frac{2\beta}{g^2}\sinh^2(gz) - \mathrm{Im}[\gamma_2 E_1(0)E_2^*(0)]\frac{1}{g}\sinh^2(2gz). \quad (14)$$

The asymmetric behavior in Fig. 2 is described by the last two terms of Eq. (14), which becomes clearer by introducing an initial phase of the waves, $E_m(0) = \hat{E}_m e^{i\varphi_m}$, and by introducing an initial phase of the waves, $E_m(0) = \hat{E}_m d^{i\varphi_m}$, and by introducing

$$\Psi = \frac{n_0\omega^2}{k_{2z}c_0^2} n_{o,e}^q \frac{\cos(\vartheta - \delta)}{-\cos\delta}, \quad (15)$$

which depends on the temperature of the liquid crystal. Further we obtain with Eq. (11)

$$\gamma_2 E_1(0)E_2^*(0) = \Psi\hat{E}_1\hat{E}_2\hat{E}_3\hat{E}_4 e^{i\sigma}, \quad (16)$$

with $\sigma = (\varphi_1 - \varphi_2) + (\varphi_4 - \varphi_3) - \Delta\vec{k}\cdot\vec{r}$.

With these abbreviations the last two terms of Eq. (14) may be expressed by

$$\mathrm{Re}[\gamma_2 E_1(0)E_2^*(0)]\frac{2\beta}{g^2}\sinh^2(gz) = \frac{2\beta\Psi}{g^2}\hat{E}_1\hat{E}_2\hat{E}_3\hat{E}_4 \times \cos\sigma\sinh^2(gz), \quad (17)$$

$$\mathrm{Im}[\gamma_2 E_1(0)E_2^*(0)]\frac{1}{g}\sinh(2gz) = \frac{\Psi}{g}\hat{E}_1\hat{E}_2\hat{E}_3\hat{E}_4 \times \sin\sigma\sinh(2gz). \quad (18)$$

The sign of these expressions depends on $\cos\sigma$ and $\sin\sigma$, respectively, and therefore on the value of σ. A change in the polarization of the signal beam from $+\xi$ to $-\xi$ changes the initial phase of the beam E_2 from φ_2 to $\varphi_2 \pm \pi$, leading to a change in the sign of $\cos\sigma$ and $\sin\sigma$, respectively. The same effect takes place with a change in the polarization of the pump beam from $+\zeta$ to $-\zeta$. The mismatch Δk must be taken into account in general, but becomes zero in the case of symmetric incident beams. The phase differences $\varphi_1 - \varphi_2$ and $\varphi_4 - \varphi_3$ are zero or a multiple of π. Therefore, we can assume with respect to our experiment $\cos\sigma \approx 1$ or -1 and $\sin\sigma \approx 0$. The power of the ordinary component of the signal beam may then be expressed by

$$P_2(z) = \hat{P}_2\left(\cosh^2(gz) + \frac{\beta^2}{g^2}\sinh^2(gz)\right) + \hat{P}_1\frac{Z_e}{Z_o}\frac{|\gamma_2|^2}{g^2}\sinh^2(gz) + \sqrt{\hat{P}_1\hat{P}_2\hat{P}_3\hat{P}_4}\,\frac{2Z_e\Psi\beta}{Ag^2}\cos\sigma\sinh^2(gz), \quad (19)$$

with A the cross section of the laser beam inside the nonlinear medium. Remember that the other case of Eq. (19) is built by replacing sinh and cosh by sin and cos. In the case of small values of gz we can further introduce the approximations $\sin(gz) = \sinh(gz) = gz$ and $\cos(gz) = \cosh(gz) = 1$.

After these calculations we are able to understand the experimental results presented in Fig. 2. In the above equation, β, γ_2, $\hat{P}_3$, and $\hat{P}_4$ depend on the angle of polarization of the pump beam. We have

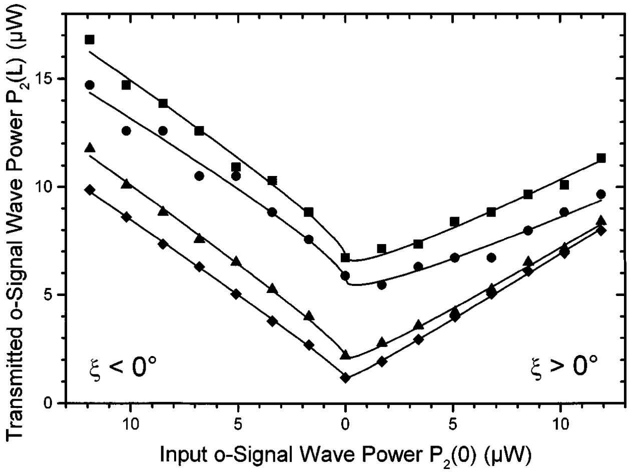

FIG. 3. Transmitted vs input o-signal wave power at different liquid crystal temperatures. From top to bottom: $T_{NI} - T = 2, 3, 5, 6.5$ °C, where $T_{NI} = 35$ °C is the phase transition temperature of 5CB. The pump beam polarization angle was fixed to $\zeta = +45°$, and the signal beam polarization was varied between $\xi = -10°$ to 10°. Solid curves display theoretical calculations of the amplification effects.

$\hat{P}_3 = \hat{P}_P \cos^2\zeta$ and $\hat{P}_4 = \hat{P}_P \sin^2\zeta$, with $\hat{P}_P$ the total pump beam power. As a good approximation we can assume $\beta \propto \hat{P}_3$, and furthermore $|\gamma_2|^2 \propto \hat{P}_3\hat{P}_4 = \frac{1}{4}\hat{P}_P^2 \sin^2(2\zeta)$. The first expression of Eq. (19) describes a power offset. The second term is proportional to $|\gamma_2|^2$ and therefore has the typical (symmetric) $\sin^2(2\zeta)$ shape, describing the diffraction of E_4 mediated by the grating formed by E_1 and E_3. The third term of Eq. (19) describes the deviation from the symmetric $\sin^2(2\zeta)$ shape and is characterized by $\sqrt{\hat{P}_3\hat{P}_4}\cos\sigma \propto \sin(2\zeta)$. Note that this deviation appears only if $\hat{P}_1$ and $\hat{P}_2$ are not zero. Note also that the sign of this deviation is determined by the $\cos\sigma$ factor. The theoretically obtained dependence fits very well with the experimental observations given in Fig. 2.

Let us now investigate the dependence of the transmitted ordinary signal beam power $P_2(L)$ from the power of the same beam at the input $\hat{P}_2$. The angle of the pump beam polarization was fixed at $\zeta = 45°$, i.e., the maximum of $P_2(L)$. Practically, we have changed the ordinary signal beam component by rotating the signal beam from $\xi = -10°$ to $+10°$. In that range the extraordinary component does not change very much. The result for different liquid crystal temperatures is shown in Fig. 3.

As a result, let us note that the transmitted power depends on the direction of the rotation of the signal beam which is a consequence of the vectorial addition of the components of the beam, as described by Eq. (19). The first term is proportional to $\hat{P}_2$ and explains the V shape of the curves. The second term gives the offset depending on the temperature of the liquid crystal. The third term leads to a component proportional to the square root of $\hat{P}_2$ which is added for $\xi < 0°$ and subtracted otherwise. The sign is given by the $\cos\sigma$ factor of each case. The fits of the experimental curves in Fig. 3 are in a good agreement with the theoretical calculations. For comparison of the experimental results with the theoretical calculations it is important to include the absorption of the liquid crystal. It is obvious that, in spite of absorption, the transmitted ordinary component of the signal beam exceeds the input at temperature above 30 °C. We therefore have an amplifier for certain components of the input wave.

In conclusion, we have proved the ability of liquid crystal media for vectorial wave mixing processes for the first time. The birefringence of the nonlinear optical medium leads to the propagation of two different wave components inside the medium, which are furthermore exposed to nonlinear coefficients of different value and sign. This allows polarization switching and amplification, which has been experimentally proved. Experimental observations are in good agreement with theoretical calculations starting from Maxwell's equations in the SVE approximation.

We want to thank Chris Scharfenorth for preparing the coatings for the liquid crystal cells. This work is supported by the Deutsche Forschungsgemeinschaft (Sfb 335).

[1] See, e.g., P. Yeh, IEEE J. Quantum Electron. **QE-25**, 484 (1989).
[2] H. J. Eichler *et al.*, Phys. Rev. A **35**, 4673 (1987).
[3] F. Sanchez, P. H. Kayoun, and J. P. Huignard, J. Appl. Phys. **64**, 26 (1988).
[4] I. C. Khoo and T. H. Liu, Phys. Rev. A **39**, 4036 (1989).
[5] V. L. Vinetskii *et al.*, Sov. Phys. Usp. **22**, 742 (1979).
[6] I. C. Khoo *et al.*, IEEE J. Quantum Electron. **QE-29**, 2972 (1993).
[7] I. C. Khoo, Phys. Rev. Lett. **64**, 2273 (1990).
[8] I. C. Khoo and N. V. Tabiryan, Phys. Rev. A **41**, 5528 (1990).
[9] I. C. Khoo, Yu Liang, and Hong Li, IEEE J. Quantum Electron. **QE-28**, 1816 (1992).
[10] M. Petrovic and M. Belic, Opt. Commun. **109**, 338 (1994).
[11] I. C. Khoo and S. T. Wu, *Optics and Nonlinear Optics of Liquid Crystals* (World Scientific Publishing Co. Pte. Ltd., Singapore, 1993).